GEOLOGICAL APPLICATIONS OF MULTIPOLARIZATION SAR DATA

Diane L. Evans
Jet Propulsion Laboratory, California Institute of Technology
Pasadena, California

Spaceborne Synthetic Aperture Radar (SAR) data acquired by Seasat and the Shuttle Imaging Radar (SIR-A/B) operating at L-band with HH polarization have been found to be useful in conjunction with other sensors for lithologic discrimination in arid environments with limited vegetation cover [1-3]. In order to assess the utility of more advanced sensors for geologic research and define the unique contributions each sensor makes, remote sensing data were collected over the Deadman Butte area of the Wind River Basin, Wyoming (Figure 1) as part of a cooperative study between the Jet Propulsion Laboratory Radar Sciences, Geology and Cartographic Applications groups, the Hawaii Institute of Geophysics, and the University of Wyoming. The Wind River Basin is an asymmetric sedimentary basin in central Wyoming created during the early Eocene Laramide orogeny. The stratigraphic section of the Deadman Butte study area, which was measured by Woodward [4] is made up of Paleozoic and Mesozoic marine shales, siltstones, limestones, and sandstones. Sensor systems included Landsat 4 Thematic Mapper (TM), Thermal Infrared Multispectral Scanner (TIMS) and the Multipolarization, L-band airborne SAR, a prototype for the next Shuttle Imaging Radar (SIR-C). Sensor parameters are given in Table 1.

Based on previous work by Kahle and Goetz [5], TIMS bands 1, 3 and 5 were processed with a decorrelation technique in order to suppress temperature differences and maximize emissivity differences related to crystalline structure in silicate minerals. All data were resampled to the TM pixel size (30m) and registered to the TM base. A rubber-sheet stretch of the data, based on a set of tiepoints, was used for the registration. The coregistered data are shown as Figure 2. In order to quantify the improvement in rock type discrimination that results from using the multisensor data over any individual data type, a Linear Discriminant Analysis was performed. The program used in this study is part of the UCLA Biomedical Data Processing Package [6] and is described by Blom and Daily [1]. Basically, areas of known rock types are selected as training areas, and means and standard deviations for each training area in each image are calculated. The program then determines which image is best for discriminating among the rock units by computing the discriminant function for each area and attempting to separate training areas into groups. Remaining images are then checked at the next step to find the next most useful for separating the training areas into groups, and so on. In this way, the multisensor images can be ranked in order of their utility for separating the units, and it is possible to determine which data set contributes to the discrimination between specific rock types.

Training areas were chosen for each of the major lithologic units outcropping in the Deadman Butte area, a dolomite member of the Phosphoria Formation, an unnamed red siltstone member of the Dinwoody Formation, the Red Peak Siltstone and Alcova Limestone members of the Chugwater Formation, the Redwater Shale Member of the Sundance Formation, and the Cloverly Sandstone,

Thermopolis Shale, Muddy Sandstone, Mowry Shale and Frontier Formation. The results of the Linear Discriminant Analysis are presented in Table 2. The increased capability to classify units using the multisensor data set over any individual sensor is shown graphically in Figure 3. Results show that classification accuracy increases with the addition of new channels up to 96% using 10 channels, with the three optimum channels being LVH, TIMS5 and TM5. The overall accuracy achieved using only the TM bands was 76%; using only TIMS, 73% and SAR alone, 62%. Thus, the multisensor data set provided at least 20% better classification accuracy than any of the individual sensors. However, it should be noted that this procedure only provides classification accuracies for the training areas themselves and may not represent the ability to classify entire rock units. The results can therefore only be used as one indicator of the optimum bandpasses. Another important factor is how well the training areas represent the various lithologies and can be used for classification, which is a topic of ongoing research.

REFERENCES

[1] Blom, R. and M. Daily, Radar image processing for rock type discrimination, IEEE Trans. on Geoscience and Remote Sensing, Vol. GE-20, no. 3, 343-351, 1982.

[2] Evan, D. L., Use of coregistered visible, infrared and radar images for geologic mapping, Spaceborne Imaging Radar Symposium, Pasadena, JPL Pub. 83-11, 1983.

[3] Rebillard, P. and D. L. Evans, Analysis of coregistered Landsat, Seasat and SIR-A images of varied terrain types, Geophysical Research Letters, Vol. 10, no. 4, 277-280, 1983.

[4] T. C. Woodward, Geology of Deadman Butte area, Natrona County, Wyoming, Bull Amer. Assoc. Petroleum Geol., Vol. 41, pp. 212-262, 1957.

[5] A. B. Kahle, and A. F. H. Goetz, Mineralogic information from a new airborne thermal infrared multispectral scanner, Science Vol. 222, 24-27, 1983.

[6] W. J. Dixon, Ed., BMD Biomedical Computer Programs, Berkeley, California: University of California Press, 1970.

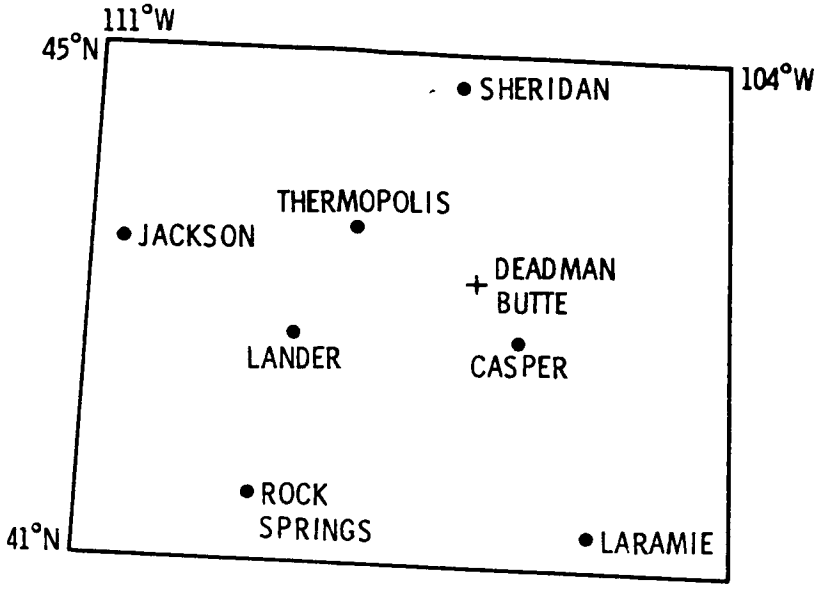

Figure 1. Location of Deadman Butte study area

Table 1. Imaging sensor systems

Sensor	TM	TIMS	Quad-pol SAR
Platform	Landsat 4 & 5	Aircraft	Aircraft
Altitude	700 km	10 km*	10 km*
Swath width	185 km	4 km*	6 km*
Wavelength	TM1: .45 - .52 μm	TIMS1: 8.1 - 8.5 μm	24.6 cm
	TM2: .52 - .60 μm		
	TM3: .63 - .69 μm	TIMS3: 8.9 - 9.3 μm	
	TM4: .76 - .90 μm		
	TM5: 1.55 - 1.75 μm	TIMS5: 10.2 - 10.9 μm	
	TM7: 2.0 - 2.36 μm		
Pixel size	30 m (.45 - 2.36 μm)	25 m*	10 m*

*Typical

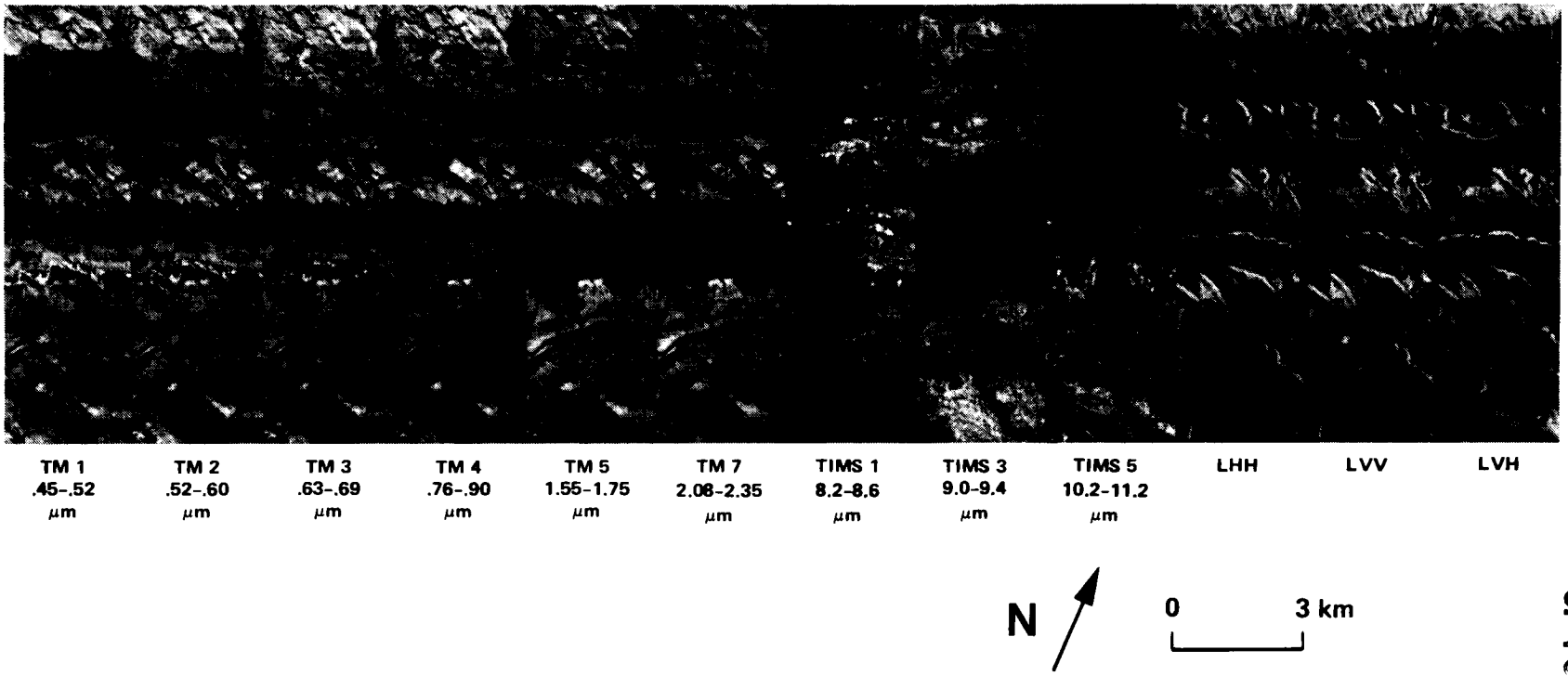

Figure 2. Multisensor data set of Deadman Butte study area

Table 2. Cumulative classification accuracy (%) ranked in order of decreasing usefulness

	LVH	TIMS5	TM5	TM2	LVV	TIMS3	TM7	TMS1	TM4	TM3	TM1	LHH
U. Frontier	57	68	80	84	85	95	94	95	95	95	95	95
L. Frontier	43	46	60	62	81	85	89	89	91	92	92	92
Mowry	55	48	60	58	87	89	88	95	99	100	100	100
Muddy	75	75	100	100	100	100	100	100	100	100	100	100
Thermopolis	33	58	97	97	100	100	100	100	100	100	98	98
Clovery	37	55	84	89	90	93	95	97	98	98	100	98
Sundance	98	98	99	98	95	95	95	95	99	98	100	100
Alcova	16	81	90	96	96	98	98	100	100	100	94	95
Chugwater	11	42	48	86	89	90	91	93	92	92	89	89
Dinwoody	63	52	59	67	85	82	82	85	86	89	92	92
Phosphoria	25	79	79	85	86	89	89	90	87	89	100	100
Average	42	64	81	84	90	92	93	94	95	96	96	96

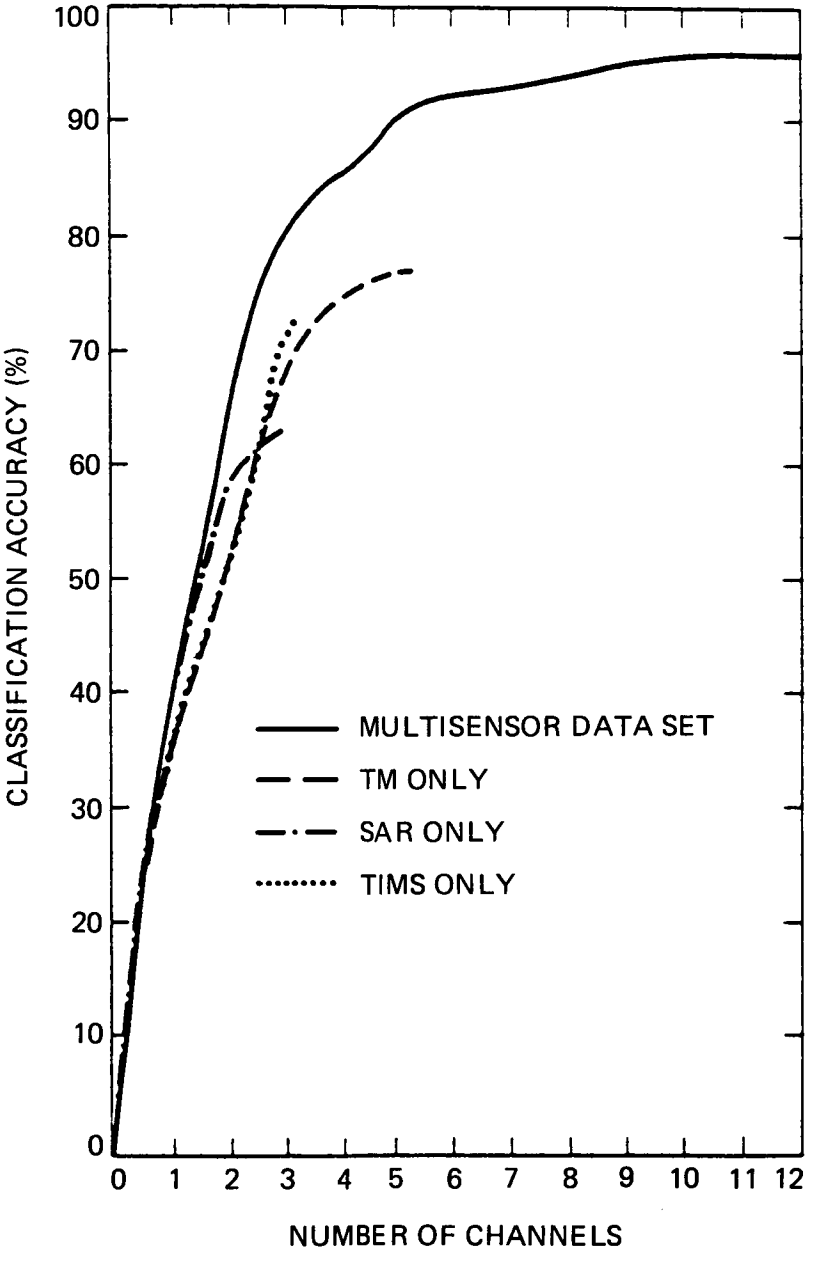

Figure 3. Improvement in classification accuracy using multisensor data set